

Superfluid instability of r-modes in “differentially rotating” neutron stars

N. Andersson¹, K. Glampedakis^{2,3} & M. Hogg¹

¹*School of Mathematics, University of Southampton,
Southampton SO17 1BJ, United Kingdom*

²*Departamento de Fisica, Universidad de Murcia, E-30100 Murcia, Spain*

³*Theoretical Astrophysics, University of Tübingen,
Auf der Morgenstelle 10, Tübingen, D-72076, Germany*

Abstract

Superfluid hydrodynamics affects the spin-evolution of mature neutron stars, and may be key to explaining timing irregularities such as pulsar glitches. However, most models for this phenomenon exclude the global instability required to trigger the event. In this paper we discuss a mechanism that may fill this gap. We establish that small scale inertial r-modes become unstable in a superfluid neutron star that exhibits a rotational lag, expected to build up due to vortex pinning as the star spins down. Somewhat counterintuitively, this instability arises due to the (under normal circumstances dissipative) vortex-mediated mutual friction. We explore the nature of the superfluid instability for a simple incompressible model, allowing for entrainment coupling between the two fluid components. Our results recover a previously discussed dynamical instability in systems where the two components are strongly coupled. In addition, we demonstrate for the first time that the system is secularly unstable (with a growth time that scales with the mutual friction) throughout much of parameter space. Interestingly, large scale r-modes are also affected by this new aspect of the instability. We analyse the damping effect of shear viscosity, which should be particularly efficient at small scales, arguing that it will not be sufficient to completely suppress the instability in astrophysical systems.

I. INTRODUCTION

Since the first observation of a glitch in the spindown of the Vela Pulsar in 1969 [1, 2], there have been a large number of similar events observed in other pulsars [3, 4]. Several competing, in some cases complimentary, mechanisms have been suggested as explanation for these occurrences [5–9]. The two most widely classes models relate either to changes in the star’s elastic crust or the dynamics of the superfluid neutrons that are present both in the core and the inner crust. The first set of models involve fractures in the crust, leading to changes in the moment of inertia of the star [10]. The second set involves the unpinning of vortices associated with a superfluid component from the star’s inner crust [11]. The unpinning event is attributed to the build-up of “differential rotation” between the two components (elastic crust and interpenetrating superfluid). It is the second of these two mechanisms with which we concern ourselves in this paper.

We consider a promising mechanism for triggering the observed events; a superfluid instability present in systems with “differential rotation”, like the lag that plays a central role in all vortex-based glitch models. The basic mechanism has already been discussed in [12], where it was argued that the instability may trigger large-scale vortex unpinning leading to the observed events. The first part of the argument was a demonstration that unstable r-modes could be generated by the difference in rotation of the charged particles (protons and electrons) and the superfluid neutrons in the star. In particular, it was shown in [12] that such unstable modes exist for a strongly coupled system. The second part of the argument consisted of a demonstration that viscosity would not suppress this instability completely, but would allow growing modes to exist for a range of wavelengths once a critical rotational lag was reached. The third part of the argument placed the mechanism in an astrophysical context by comparing the predictions of the model to observational data.

In this paper we consider this new r-mode instability in more detail. We extend the analysis of [12] beyond the strong-drag limit, and show that dynamically unstable modes (with a growth time similar to the star’s rotation rate) exist for a wide range of parameter values. In addition, we discover that the r-modes also suffer a secular instability (with growth time proportional to the mutual friction) throughout much of parameter space. This aspect is new. It is particularly interesting as it affects also the global scale r-modes, while the dynamical instability is restricted to small scale modes. As in the previous work, we

limit ourselves to discussion of the non-relativistic case. Again following the approach of [12], we introduce shear viscosity and demonstrate that the instability is not completely suppressed by the inclusion of the associated damping.

The main purpose of this investigation is to establish the robustness of the superfluid instability, highlight the key ingredients that lead to its presence and set the stage for more detailed studies of this mechanism. The instability that we consider may be generic (belonging to the class of two-stream instabilities that are known to operate in a wide variety of physical systems [13]), but at this point it is not clear how it is affected by other aspects of neutron star physics. In particular, future work needs to extend the analysis to account for the crust elasticity and the presence of the star’s magnetic field.

II. SETTING THE STAGE

We consider the conditions that are expected to prevail in the outer core of a mature neutron star, where a neutron superfluid is thought to coexist with a proton superconductor. A key qualitative aspect of this system is that it allows the two “fluids” to flow “independently”, leading to dynamics that is well represented by a two-fluid model. In order to keep the analysis manageable, we assume that both fluid components are charge neutral. This allows us to neglect (in this first proof-of-principle analysis) the star’s magnetic field. This is obviously a severe simplification, but to analyse the full problem would be difficult at this point. The key aspect that we add to previous studies in this problem area is the relative rotation between the two components, expected to build up as the observed component spins down due braking associated with the exterior magnetic field. We are interested in the global oscillations of a star that exhibits this kind of “differential” rotation. Despite this being a key aspect of the generally accepted “explanation” for observed pulsar glitches, there have not yet been any detailed studies of the dynamics of such a system. In this sense, the present work provides an important step towards realism.

The main question that motivates us stems from the discovery that two-stream instabilities are generic in the two-fluid model [14]. Given this, it is relevant to ask whether the rotational lag that builds up in a mature neutron star may lead to such instabilities and, if so, what the observational consequences may be. Conversely, given that we do not yet know what the mechanism that triggers the observed glitches may be, but that it ought to be

some kind of “global” instability, it is interesting to ask whether the two-stream instability may be relevant in this context.

We consider the linear perturbations of a system that exhibits a rotational lag. Because of this set-up, it is natural to work in the inertial frame (rather than choosing one of the rotating frames). It is also natural, given the complex nature of the perturbed velocity fields etcetera to carry out the analysis in a coordinate basis. This means that vectors, like the velocity, are expressed in terms of their components, v^i (say), and a distinction is made between co- and contravariant objects, with the former following from the latter as $v_i = g_{ij}v^j$ where g_{ij} is the flat three-dimensional metric. This description of the problem is also advantageous since it involves the use of the covariant derivative ∇_i associated with the given metric, which automatically encodes the scale factors associated with the curvilinear coordinates (r, θ, φ) that are appropriate for the problem.

We consider a system with two interpenetrating fluids, labeled n and p (from now on), which are assumed to rotate rigidly in such a way that

$$v_x^i = \Omega_x \hat{e}_\varphi^i \quad , \quad x = n, p \quad (1)$$

where \hat{e}_φ^i represents the azimuthal basis vector (and \hat{e}_θ^i later the polar one). The angular velocities, Ω_x , are assumed to be constant, but we allow for differential rotation, i.e. $\Omega_n^i \neq \Omega_p^i$. To keep the analysis tractable, we assume that the two rotation axes coincide, and use

$$\Omega_p^i = \Omega^i \quad , \quad \text{and} \quad \Omega_n^i = (1 + \Delta)\Omega^i \quad (2)$$

Making contact with pulsar observations, Ω^i would be the observed (angular) rotation frequency (i.e. that of the crust) while Ω_n^i represents the rotation of the unseen (interior) superfluid component. As the superfluid is expected to lag behind as the crust spins down, one would typically expect Δ to be small (of the order of 10^{-4} at the time of a glitch [3]) and positive.

Key to understanding the dynamics of glitching pulsars is the appreciation that the neutrons may form Cooper pairs, and hence act as a superfluid. The upshot of this is that bulk rotation can only be achieved by the formation of an array of quantized vortices. As discussed in, for example, [15] the quantization condition is imposed on the momentum that is conjugate to the velocity v_n^i . This momentum is given by

$$p_i^n = m_p (v_i^n + \varepsilon_n w_i^{pn}) \quad (3)$$

where m_p is the nucleon mass (we ignore the small difference between the bare neutron and proton masses), ε_n represents the entrainment between neutrons and protons (more of which later) and the relative velocity is

$$w_{yx}^i = v_y^i - v_x^i, \quad y \neq x \quad (4)$$

Given this, and the relevant quantization condition (see [15] for discussion), the local vortex density (per unit area), n_v , follows from

$$n_v \kappa^i = \epsilon^{ijk} \nabla_j [v_k^n + \varepsilon_n w_k^{pn}] = 2[\Omega_n^i + \varepsilon_n(\Omega_p^i - \Omega_n^i)] = 2[1 + (1 - \varepsilon_n)\Delta]\Omega^i \quad (5)$$

where κ^i is the vector aligned with the vortex array with magnitude $\kappa = h/2m_p$ (h is Planck's constant). Here we have introduced yet another simplifying assumption; we have taken the fluids to be incompressible which implies that the entrainment coefficient may (at least in the small Δ case that we are focussing on) be taken to be constant. It is also worth noting that $\rho_n \varepsilon_n = \rho_p \varepsilon_p$ where $\rho_x = m_p n_x$ are the respective mass densities.

Let us now consider the linear perturbations (represented by δ) of this kind of configuration. Assuming that the flow is incompressible also at this level (incidentally not a bad approximation for the inertial flows that we will consider) we have, first of all,

$$\nabla_i \delta v_x^i = 0 \quad (6)$$

Meanwhile, the perturbed momenta

$$\delta p_i^x = \delta v_i^x + \varepsilon_x \delta w_i^{yx} \quad (7)$$

are governed by the Euler equations;

$$\mathcal{E}_i^x = i\omega \delta p_i^x + \delta v_x^j \nabla_j p_i^x + v_x^j \nabla_j \delta p_i^x + \varepsilon_x (\delta w_j^{yx} \nabla_i v_x^j + w_j^{yx} \nabla_i \delta v_x^j) + \nabla_i \delta \Psi_x = \delta f_i^x \quad (8)$$

where

$$\Psi_x = \Phi + \tilde{\mu}_x \quad (9)$$

combines the gravitational potential Φ and the chemical potential $\tilde{\mu}_x = \mu_x/m_p$ for each fluid. We have assumed that the time-dependence is harmonic, $\propto \exp(i\omega t)$, as we are interested in the oscillation modes of the system. Later, we will make extensive use of the equations that govern the perturbed vorticity. Specifically, we will work with the quantity

$$\mathcal{W}_x^i = \epsilon^{ijk} \nabla_j \mathcal{E}_k^x \quad (10)$$

The right-hand side of (8) can be used to account for any “external” forces acting on the fluids. It can also be used to incorporate interactions between them. The main such interaction force is the mutual friction that arises due to the presence of the quantized vortices [16, 17]. The unperturbed force takes the form [18]

$$f_i^x = \frac{\rho_n}{\rho_x} \mathcal{B}' n_v \epsilon_{ijk} \kappa^j w_{xy}^k + \frac{\rho_n}{\rho_x} \mathcal{B} n_v \epsilon_{ijk} \hat{\kappa}^j \epsilon^{klm} \kappa_l w_m^{xy} \quad (11)$$

where \mathcal{B} and \mathcal{B}' are coefficients to be determined from microphysics. In the standard scenario these coefficients can be expressed in terms of a single resistivity \mathcal{R} , associated with scattering off of the vortices, such that [18]

$$\mathcal{B} = \frac{\mathcal{R}}{1 + \mathcal{R}^2} \quad (12)$$

and

$$\mathcal{B}' = \frac{\mathcal{R}^2}{1 + \mathcal{R}^2} \quad (13)$$

The weak- and strong coupling limits discussed later correspond to, respectively, $\mathcal{R} \rightarrow 0$ and $\mathcal{R} \rightarrow \infty$. It is worth noting that the system can build up a differential rotation lag only as long as some additional force (like vortex pinning) prevents the mutual friction from acting. The presence of such a force is implicitly assumed in the following discussion.

Perturbing (11), we get

$$\begin{aligned} \delta f_i^x = \frac{\rho_n}{\rho_x} \mathcal{B}' & \left[\delta(n_v \kappa^j) \epsilon_{ijk} w_{xy}^k + n_v \kappa^j \epsilon_{ijk} \delta w_{xy}^k \right] \\ & + \frac{\rho_n}{\rho_x} \mathcal{B} \epsilon_{ijk} \epsilon^{klm} \left[\delta(n_v \kappa_l) \hat{\kappa}^j w_m^{xy} + n_v \kappa_l (w_m^{xy} \delta \hat{\kappa}^j + \hat{\kappa}^j \delta w_m^{xy}) \right] \end{aligned} \quad (14)$$

To evaluate this we need

$$\delta(n_v \kappa^i) = \epsilon^{ijk} \nabla_j \delta p_k^n \quad (15)$$

and

$$\delta \hat{\kappa}^i = \frac{1}{n_v \kappa} (\delta_j^i - \hat{\kappa}^i \hat{\kappa}_j) \epsilon^{jlm} \nabla_l \delta p_m^n \quad (16)$$

where $\hat{\kappa}^i$ is a unit vector aligned with κ^i , together with, cf. (5),

$$n_v \kappa = 2[1 + (1 - \varepsilon_n) \Delta] \Omega \quad (17)$$

In the perturbation equations discussed in the next section, we will not work with the momentum equations (8) directly. Rather, we use two combinations that represent the total

(perturbed) momentum and the difference. It is well established that these combinations isolate the two dynamical degrees of freedom in an “uncoupled” two-fluid system [19]. Hence, this decomposition is often used in studies of oscillating superfluid neutron stars [20]. This means that we need;

$$\rho_n \delta f_i^n + \rho_p \delta f_i^p = 0 \quad (18)$$

and

$$\delta f_i^p - \delta f_i^n = -\frac{1}{x_p} \delta f_i^n \quad (19)$$

where we have introduced the proton fraction $x_p = \rho_p / (\rho_n + \rho_p)$. Only the second degree of freedom is explicitly affected by the mutual friction.

Finally, we want to account for the presence of shear viscosity (in the superfluid case mainly due to electron-electron scattering). In the incompressible case, this means that we add a force to (the right-hand side of) the proton equation of form;

$$\delta f_{sv}^i = \nu_{ee} \nabla^2 \delta v_p^i \quad (20)$$

where ν_{ee} is the kinematic viscosity coefficient. We ignore bulk viscosity for two reasons. First of all, glitching pulsars are cold enough that shear viscosity should be the dominant damping mechanism. Secondly, the particular class of fluid motion that we consider is not efficiently damped by bulk viscosity, anyway [32].

III. THE AXIAL PERTURBATION EQUATIONS

Despite the various simplifying assumptions, the general perturbation problem is challenging. It is well-known that, even in the slow-rotation limit where the star remains spherical, there exists a class of inertial modes [22] which require the coupling of many (spherical harmonics) multipoles for their description. We are, however, not going to attempt to solve the general problem. Instead we will ask a very specific question; How does the presence of the rotational lag affect the r-modes of the system? This question is relevant for a number of reasons, perhaps the most important being related to the fact that the large scale r-modes may be driven unstable by the emission of gravitational radiation [32]. From a practical point-of-view, it is natural to focus on the r-modes since they are associated with particularly simple velocity fields. The hope would be that the corresponding problem remains tractable even when we add the rotational lag.

The r-modes are a subclass of inertial modes (restored by the Coriolis force) that are purely axial/toroidal to leading order. This means that the perturbed velocities take the form

$$\delta v_{\mathbf{x}}^i = -\frac{im}{r^2 \sin \theta} U_{\mathbf{x}}^l Y_l^m \hat{e}_{\theta}^i + \frac{1}{r^2 \sin \theta} U_{\mathbf{x}}^l \partial_{\theta} Y_l^m \hat{e}_{\varphi}^i \quad (21)$$

where $Y_l^m(\theta, \varphi)$ are the standard spherical harmonics, $U_{\mathbf{x}}^l(r)$ are the mode amplitudes, and the symmetry of the problem is such that the m -multipoles (proportional to $e^{im\varphi}$) decouple. In the single (barotropic) fluid case, r-mode solutions exist for each individual $l = m \geq 1$. The main focus in previous work has been on the quadrupole mode ($l = 2$) since it is associated with the fastest growing gravitational-wave instability [32]. In this work we will end up studying a large range of scales, including small scale modes with l the order of 100. In a neutron star, such perturbations would be relatively local, corresponding to a typical lengthscale of 100 m.

As hinted at in the previous section, we prefer to work with slightly different perturbation variables. Experience from other problems involving the two-fluid model [20] suggests that it is advantageous to work with the total perturbed momentum flux, defined as

$$\rho U^l = \rho_{\mathbf{n}} U_{\mathbf{n}}^l + \rho_{\mathbf{p}} U_{\mathbf{p}}^l \quad (22)$$

with $\rho = \rho_{\mathbf{n}} + \rho_{\mathbf{p}}$. We take the second variable to be given by the velocity difference;

$$u^l = U_{\mathbf{p}}^l - U_{\mathbf{n}}^l \quad (23)$$

In order to “simplify” the final perturbation equations it is useful to express the frequency in the “rotating frame”, i.e. work with σ defined by

$$\omega + m\Omega = \sigma\Omega \quad (24)$$

It is also convenient to introduce

$$L = l(l+1) \quad (25)$$

$$Z = 1 - x_{\mathbf{p}} - \varepsilon_{\mathbf{p}} \quad (26)$$

and

$$\bar{Z} = \frac{x_{\mathbf{p}} Z}{1 - x_{\mathbf{p}}} \quad (27)$$

Finally, we use (as in [20]) the scaled mutual friction coefficients;

$$\bar{\mathcal{B}}' = \mathcal{B}'/x_{\mathbf{p}} , \quad \text{and} \quad \bar{\mathcal{B}} = \mathcal{B}/x_{\mathbf{p}} \quad (28)$$

The perturbation equations can now be obtained by inserting the expected velocity field in the equations from the previous section. After some manipulations this leads to the following set of the equations to be solved: From $\rho_n \mathcal{W}_n^r + \rho_p \mathcal{W}_p^r$ we, first of all, get

$$[L\sigma - 2m] U^l Y_l^m = -m\Delta(L - 2)[U^l - \bar{Z}u^l]Y_l^m \quad (29)$$

(Here, and in the following, summation over $l \geq m$ is implied.) The advantage of working with this combination, that represents to total vorticity, is that there are no mutual friction terms in the equation. Such terms are associated with the relative flow. To see this we consider the combination $\mathcal{W}_p^r - \mathcal{W}_n^r$, leading to

$$\begin{aligned} & \left[\frac{L\sigma\bar{Z}}{x_p} - 2m(1 - \bar{\mathcal{B}}') - 2i\bar{\mathcal{B}}(L - m^2) \right] u^l Y_l^m = \\ & = -m\Delta \left\{ \frac{[(L - 4)x_p + 2]\bar{Z}}{x_p} - 2(1 - x_p) \right\} u^l Y_l^m + m\Delta \left(L - \frac{2\bar{Z}}{x_p} \right) U^l Y_l^m \\ & \quad + m\Delta L\bar{\mathcal{B}}'(\bar{Z}u^l - U^l)Y_l^m - 2m\bar{\mathcal{B}}'\Delta(\bar{Z} + 1 - x_p)u^l Y_l^m \\ & \quad + i\bar{\mathcal{B}}\Delta L[\bar{Z}(r\partial_r u^l - u^l) - r\partial_r U^l + U^l]Y_l^m + 2i\bar{\mathcal{B}}\Delta(L - m^2)(\bar{Z} + 1 - x_p)u^l Y_l^m \\ & \quad + i\bar{\mathcal{B}}L\Delta[r\partial_r U^l - 3U^l - \bar{Z}(r\partial_r u^l - 3u^l)]\cos^2\theta Y_l^m \\ & \quad + i\bar{\mathcal{B}}\Delta[2r\partial_r U^l - LU^l - \bar{Z}(2r\partial_r u^l - Lu^l)]\cos\theta\sin\theta\partial_\theta Y_l^m \quad (30) \end{aligned}$$

We will also use the radial components of the Euler equations. From the combination $\rho_n \mathcal{E}_n^r + \rho_p \mathcal{E}_p^r$ we find

$$\begin{aligned} & [x_p r\partial_r \delta\Psi_p^l + (1 - x_p)r\partial_r \delta\Psi_n^l]Y_l^m - 2\Omega U^l \sin\theta\partial_\theta Y_l^m = \\ & = -\Delta\Omega(1 - x_p)[(x_p - \bar{Z})r\partial_r u^l + 2\bar{Z}u^l - 2U^l]\sin\theta\partial_\theta Y_l^m \quad (31) \end{aligned}$$

while $\mathcal{E}_p^r - \mathcal{E}_n^r$ leads to

$$\begin{aligned} & (r\partial_r \delta\Psi_p^l - r\partial_r \delta\Psi_n^l)Y_l^m - 2\Omega(1 - \bar{\mathcal{B}}')u^l \sin\theta\partial_\theta Y_l^m - 2im\bar{\mathcal{B}}\Omega u^l \cos\theta Y_l^m = \\ & = -\Delta\Omega \left\{ \left(1 - \frac{\bar{Z}}{x_p} \right) r\partial_r U^l + \frac{2\bar{Z}}{x_p} U^l + (1 - 2x_p) \left[\left(1 - \frac{\bar{Z}}{x_p} \right) r\partial_r u^l + \frac{2\bar{Z}}{x_p} u^l \right] \right. \\ & \quad \left. - 2(1 - x_p)u^l \right\} \sin\theta\partial_\theta Y_l^m \\ & \quad + \bar{\mathcal{B}}'\Delta\Omega[r\partial_r U^l - \bar{Z}r\partial_r u^l - 2(1 - x_p + \bar{Z})u^l]\sin\theta\partial_\theta Y_l^m \\ & \quad + im\bar{\mathcal{B}}\Delta\Omega[r\partial_r U^l - \bar{Z}r\partial_r u^l + 2(1 - x_p + \bar{Z})u^l]\cos\theta Y_l^m \quad (32) \end{aligned}$$

Finally, it is convenient to work with a “divergence equation” [20] that follows from the combination

$$\begin{aligned}
& \sin \theta \partial_\theta [\sin \theta (\rho_n \mathcal{E}_n^\theta + \rho_p \mathcal{E}_p^\theta)] + \partial_\varphi [\rho_n \mathcal{E}_n^\varphi + \rho_p \mathcal{E}_p^\varphi] \longrightarrow \\
& -L[x_p \delta \Psi_p^l + (1 - x_p) \delta \Psi_n^l] Y_l^m + 2\Omega U^l [L \cos \theta Y_l^m + \sin \theta \partial_\theta Y_l^m] = \\
& = -\Delta \Omega (1 - x_p) \{ 2U^l [L \cos \theta Y_l^m + \sin \theta \partial_\theta Y_l^m] - L x_p u^l [2 \cos \theta Y_l^m + \sin \theta \partial_\theta Y_l^m] \\
& \quad + (L - 2) \bar{Z} u^l \sin \theta \partial_\theta Y_l^m \} \quad (33)
\end{aligned}$$

Analogously, we consider the “difference” equation;

$$\begin{aligned}
& \sin \theta \partial_\theta [\sin \theta (\mathcal{E}_p^\theta - \mathcal{E}_n^\theta)] + \partial_\varphi [\mathcal{E}_p^\varphi - \mathcal{E}_n^\varphi] \longrightarrow \\
& L(\delta \Psi_n - \delta \Psi_p) Y_l^m + 2\Omega (1 - \bar{B}') u^l [L \cos \theta Y_l^m + \sin \theta \partial_\theta Y_l^m] \\
& \quad + 2im\Omega \bar{B} u^l [2 \cos \theta Y_l^m + \sin \theta \partial_\theta Y_l^m] = \\
& = \Delta \Omega L (U^l - x_p u^l) [2 \cos \theta Y_l^m + \sin \theta \partial_\theta Y_l^m] \\
& - \Delta \Omega \left[\frac{(L - 2) \bar{Z}}{x_p} (U^l + u^l) - (L - 2)(1 - x_p + 2\bar{Z}) u^l \right] \sin \theta \partial_\theta Y_l^m \\
& + \Delta \Omega \bar{B}' \{ -LU^l + [2(Z + x_p) - (1 - x_p)] Lu^l \} [2 \cos \theta Y_l^m + \sin \theta \partial_\theta Y_l^m] \\
& \quad - \Delta \Omega \bar{B}' (L - 2)(Z + x_p) u^l \sin \theta \partial_\theta Y_l^m \\
& \quad - 2im\Omega \bar{B} \Delta (x_p + Z) u^l [2 \cos \theta Y_l^m + \sin \theta \partial_\theta Y_l^m] \\
& \quad - im\Omega \bar{B} \Delta [2r \partial_r U^l + LU^l + (1 - 2x_p - Z)(2r \partial_r u^l + Lu^l)] \cos \theta Y_l^m \quad (34)
\end{aligned}$$

Next, we separate the l -multipoles by means of the standard recurrence relations

$$\cos \theta Y_l^m = Q_{l+1} Y_{l+1}^m + Q_l Y_{l-1}^m \quad (35)$$

and

$$\sin \theta \partial_\theta Y_l^m = l Q_{l+1} Y_{l+1}^m - (l + 1) Q_l Y_{l-1}^m \quad (36)$$

where

$$Q_l^2 = \frac{(l - m)(l + m)}{(2l - 1)(2l + 1)} \quad (37)$$

These relations lead to

$$\cos^2 \theta Y_l^m = (Q_{l+1}^2 + Q_l^2) Y_l^m + Q_{l+1} Q_{l+2} Y_{l+2}^m + Q_l Q_{l-1} Y_{l-1}^m \quad (38)$$

and

$$\cos \theta \sin \theta \partial_\theta Y_l^m = [l Q_{l+1}^2 - (l + 1) Q_l^2] Y_l^m + l Q_{l+1} Q_{l+2} Y_{l+2}^m - (l + 1) Q_l Q_{l-1} Y_{l-2}^m \quad (39)$$

It should be quite clear at this point that the problem we consider is rather complex, even for purely axial modes. One must also be careful, because it is not clear from the outset that modes of this particular character exists (as, in principle, rotation would couple the axial/toroidal degree of freedom to the polar/spheroidal one [22]). However, in the particular case that we are considering the problem simplifies in an almost miraculous fashion. We do not expect this level of simplification in a more general situation, leaving the problem exceedingly difficult.

IV. THE UNSTABLE R-MODES

The r-modes are very special members of the general class of inertial modes, because their eigenfunctions “truncate” at $l = m$ (at least in the standard single-fluid setting) making their eigenfunctions particularly simple (generic inertial modes involve coupling a number of $l \geq m$ multipoles [22]). Inspired by the fact that this remains true also for co-rotating superfluids [20], it makes sense to ask whether it may be the case when a rotational lag is present as well. Somewhat to our surprise, it turns out that such simple r-mode solutions do, indeed, exist. Moreover, we find that these modes may become unstable once the vortex mediated mutual friction is accounted for.

Assuming that the perturbed velocity fields take the same form as in the co-rotating case, i.e.

$$U_x^l = \begin{cases} A_x r^{m+1} & \text{for } l = m \\ 0 & \text{for } l \geq m \end{cases} \quad (40)$$

and noting that $Q_{l=m} = 0$, the equations from the previous section collapse to two scalar relations for the amplitudes. Expressing these in terms of U^m and u^m , we have

$$\begin{aligned} [(m+1)\sigma - 2 + \Delta(1 - x_p)(m-1)(m+2)]U^m \\ - (1 - x_p - \varepsilon_p)\Delta x_p(m-1)(m+2)u^m = 0 \end{aligned} \quad (41)$$

and

$$\begin{aligned}
& - \left[(m-1)(m+2) + 2\bar{\varepsilon} - m(m+1)(\bar{\mathcal{B}}' + i\bar{\mathcal{B}}) \right] \Delta U^m \\
& + \left\{ (1 - \bar{\varepsilon})(m+1)\sigma - 2(1 - \bar{\mathcal{B}}' + i\bar{\mathcal{B}}) + \Delta x_p(m-1)(m+2) \right. \\
& \left. - \bar{\varepsilon}\Delta \left\{ [m(m+1) - 4]x_p + 2 \right\} - m(m+1)\Delta x_p(1 - \bar{\varepsilon})(\bar{\mathcal{B}}' + i\bar{\mathcal{B}}) + 2(1 - \varepsilon_n)(\bar{\mathcal{B}}' - i\bar{\mathcal{B}})\Delta \right\} u^m = 0
\end{aligned} \tag{42}$$

where we have used $\bar{\varepsilon} = \varepsilon_n/x_p = \varepsilon_p/(1 - x_p)$. In the present case, where all the coefficients are taken to be constant, it is easy to see that the problem reduces to a quadratic for σ . The general solution to this quadratic is, however, rather messy and not particularly instructive. In order to understand the nature of the solutions, it is better to focus on simplified cases.

A. Dynamical instability

Let us first consider the case of vanishing entrainment. In this case we have

$$(m+1)^2\sigma^2 + P_1\sigma + P_0 = 0 \tag{43}$$

with

$$\begin{aligned}
P_0 &= 2(m-1)(m+2) (\bar{\mathcal{B}}' - i\bar{\mathcal{B}}) \Delta^2 + 4 \left[1 - (1 + x_p) (\bar{\mathcal{B}}' - i\bar{\mathcal{B}}) \right] \\
&+ 2\Delta \left[(m-1)(m+2)(x_p\bar{\mathcal{B}}' - 1) + (\bar{\mathcal{B}}' - i\bar{\mathcal{B}}) (m^2 + m - 4) + ix_p\bar{\mathcal{B}}(m^2 + m + 2) \right]
\end{aligned} \tag{44}$$

and

$$\begin{aligned}
P_1 &= (m+1) \left\{ -4 + 2(1 + x_p) (\bar{\mathcal{B}}' - i\bar{\mathcal{B}}) \right. \\
&\quad \left. + \Delta \left[2(\bar{\mathcal{B}}' - i\bar{\mathcal{B}}) + (m-1)(m+2)(1 - x_p\bar{\mathcal{B}}') - ix_p\bar{\mathcal{B}}(m^2 + m + 2) \right] \right\}
\end{aligned} \tag{45}$$

The explicit solutions are, of course, still not transparent. However, if we consider the limit of strong mutual friction coupling ($\mathcal{R} \rightarrow \infty$), such that $\mathcal{B} \approx 0$ and $\mathcal{B}' \approx 1$, then we obtain the roots

$$\sigma = -\frac{1}{(m+1)x_p} \left[1 - x_p + \Delta \pm \mathcal{D}^{1/2} \right] \tag{46}$$

with

$$\mathcal{D} = (1 + x_p)^2 + 2\Delta \{ 1 + x_p [3 - m(m+1)] \} \tag{47}$$

These solutions highlight one of the main new results in this paper (and [12]): For $m \gg 1$ we have

$$\mathcal{D} \approx (1 + x_p)^2 - 2x_p m^2 \Delta, \quad (48)$$

showing that we have *unstable* r-modes ($\text{Im } \sigma < 0$) for

$$m \gtrsim m_c, \quad \text{where} \quad m_c = \frac{1 + x_p}{\sqrt{2x_p \Delta}} \quad (49)$$

Expressed in terms of the (observed) rotation period $P = 2\pi/\Omega$ of the system, the growth timescale for these unstable modes is

$$\tau_{\text{grow}} \approx \frac{mP}{2\pi} \left(\frac{x_p}{1 + x_p} \right) \left(\frac{m^2}{m_c^2} - 1 \right)^{-1/2} \quad (50)$$

For $m \gg m_c$ (in practice, $m \gtrsim 2m_c$), the growth rate is well approximated by

$$\tau_{\text{grow}} \approx \frac{P}{2\pi} \left(\frac{x_p}{2\Delta} \right)^{1/2} \Rightarrow \tau_{\text{grow}} \approx 3 \left(\frac{x_p}{0.05} \right)^{1/2} \left(\frac{10^{-4}}{\Delta} \right)^{1/2} P \quad (51)$$

With the same scaling, the critical multipole beyond which the instability is present is

$$m_c \approx 300 \left(\frac{x_p}{0.05} \right)^{-1/2} \left(\frac{\Delta}{10^{-4}} \right)^{-1/2} \quad (52)$$

The presence of this critical value, and the associated emergence of unstable modes, is illustrated in Figure 1. We see that the instability sets in as two r-modes merge at a critical scale represented by m_c . This is the characteristic behaviour of a dynamical instability in a non-dissipative system [23].

Accounting for the entrainment obviously complicates the analysis. However, the result remains transparent in the strong coupling limit. Again setting $\mathcal{B} = 0$ and $\mathcal{B}' = 1$, we find the roots

$$\sigma = \frac{\gamma}{(m+1)x_p} \left[-(1 + \varepsilon_n) + (1 - \varepsilon_n)(x_p - \Delta) \pm \mathcal{D}^{1/2} \right] \quad (53)$$

with

$$\gamma = (1 - \varepsilon_n - \varepsilon_p)^{-1} \quad (54)$$

and

$$\begin{aligned} \mathcal{D} = \left(1 + \frac{x_p}{\gamma} \right)^2 + 2(1 - \varepsilon_n) \left[1 - (m^2 + m - 3) \frac{x_p}{\gamma} \right] \Delta \\ + (1 - \varepsilon_n)^2 \left[1 - \frac{2x_p}{\gamma} (m+2)(m-1) \right] \Delta^2 \end{aligned} \quad (55)$$

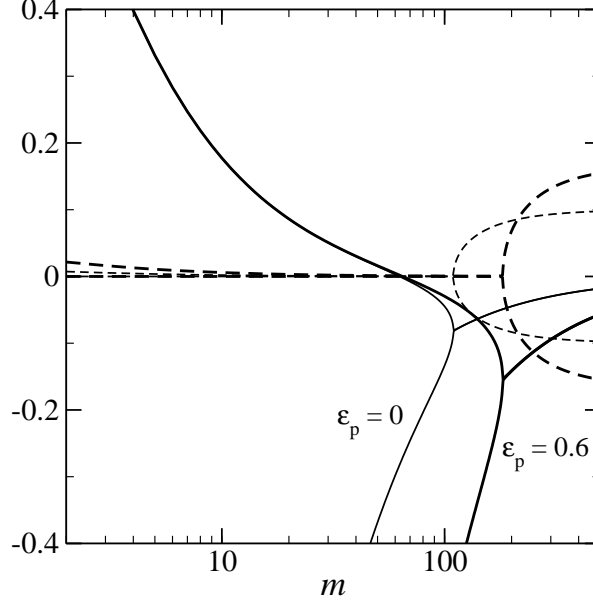


FIG. 1: Real (solid lines) and imaginary parts (dashed) of the roots to the dispersion relation (the r-modes) in the strong-coupling limit, $\mathcal{R} = 10^3$, for two illustrative cases, when $\varepsilon_p = 0$ (thin lines) and $\varepsilon_p = 0.6$ (thick lines). The rotational lag is fixed to $\Delta = 5 \times 10^{-4}$. In each case, the presence of a critical value for the azimuthal index m_c , beyond which the modes are unstable (the roots are complex) is apparent. The results also demonstrate how the entrainment affects the range of the instability by shifting m_c . Meanwhile, the growth rate of the instability (the magnitude of the imaginary part in the unstable regime) is not affected much.

For $m \gg 1$ and $\Delta \ll 1$ this is approximately,

$$\mathcal{D} \approx \frac{(\gamma + x_p)^2}{\gamma^2} \left(1 - \frac{m^2}{m_c^2} \right), \quad \text{where} \quad m_c^2 = \frac{(\gamma + x_p)^2}{2x_p \Delta \gamma (1 - \varepsilon_n)} \quad (56)$$

We see that, in this case there are unstable modes with growth time;

$$\tau_{\text{grow}} \approx \frac{mP}{2\pi} \left(\frac{x_p}{\gamma + x_p} \right) \left(\frac{m^2}{m_c^2} - 1 \right)^{-1/2} \quad (57)$$

For $m \gg m_c$ this reduces to

$$\tau_{\text{grow}} \approx \frac{P}{2\pi} \left(\frac{x_p}{2\Delta} \right)^{1/2} \epsilon_\star^{1/2} \quad (58)$$

where we have introduced

$$\epsilon_\star = \frac{1 - \varepsilon_n - \varepsilon_p}{1 - \varepsilon_n} \approx \frac{m_p^*}{m_p} \quad (59)$$

Given that a typical range of values for the effective proton mass, m_p^* , in a neutron star core is expected to be in the range $m_p^*/m_p \approx 0.5 - 0.9$ [28] we conclude that entrainment has a minor impact on the growth timescale. An illustration of this result is provided in Figure 1.

In summary, these results show that, for the typical magnitude of rotational lag inferred from radio pulsar glitches [3] we would have unstable modes with a characteristic horizontal length-scale of tens to hundreds of metres. Smaller scale r-modes would be unstable, with a growth time as fast as a few rotation periods. As the unstable modes grow extremely fast compared to the evolutionary timescale (spin-down, cooling etc) of the system it seems reasonable to expect that they may affect any real system that develops the required lag, Δ . It is worth noting that the predicted growth time is much shorter than the current observational constraint for the rise of pulsar glitches (tens of seconds [24]), unless the star is slowly rotating. Hence, the instability could grow fast enough to serve as trigger for the observed events.

B. Secular instability

Having established the existence of an instability in the strong-coupling limit, let us consider the problem for less “extreme” parameters. It is, of course, straightforward to solve (43) for given parameter values. A sample of results obtained by considering the problem for fixed \mathcal{R} , leading to the mode frequencies depending on m , are provided in Figs. 2–4. These graphs show the behaviour of the r-mode solutions as \mathcal{R} decreases from 100 to 2, i.e. as we move away from the strong-coupling regime. The results are very interesting. First of all, we see that the general trend of a “dynamical” instability (associated with modes with a markedly larger imaginary part to their frequency) setting in near the critical value m_c remains down to $\mathcal{R} = 10$ or so. For smaller values, e.g. $\mathcal{R} = 2$ as in Fig. 4, there is no longer a clear change in the imaginary part near m_c . We also see that, away from the extreme strong coupling limit the dissipative aspect of the mutual friction becomes important. In particular, it leads to the dynamical instability no longer being associated with exact mode mergers. Rather, the instability sets in at “near misses” in the complex frequency plane. This is probably what should be expected. Another aspect of the results was not expected. Considering the imaginary parts of the roots in more detail (the right-hand panels of Figs. 2–4) we see that neither imaginary part changes sign in the displayed interval (as we show $\log |\text{Im } \sigma|$ a sign change would show up as a sharp singularity). This demonstrates the most interesting new result in this paper. As we know that one of the modes is unstable beyond m_c we must conclude from Figs. 2–4 that this mode is, in fact, unstable for all lower

values of m , as well. Of course, for smaller m the growth time of the unstable modes is much longer. Later we will demonstrate that it is linked to the mutual friction parameters, making this a secular instability (plausibly related to the Donnelly-Glaberson vortex instability in laboratory superfluids [25–27]). Particularly interesting may be the fact that this instability is not restricted to the small scale r-modes. It is also active for the large scale modes. This is interesting since these modes, especially the $m = 2$ r-mode, are also secularly unstable due to gravitational-wave emission. Basically, our results show that the mutual friction may not provide damping of these modes. Rather, it could provide an additional driving mechanism for the instability. It may also be, given the strong scaling of the gravitational radiation reaction with the modes oscillation frequency (essentially the star’s spin rate) that the mutual friction driven instability dominates for slowly rotating systems. We will return to this question later.

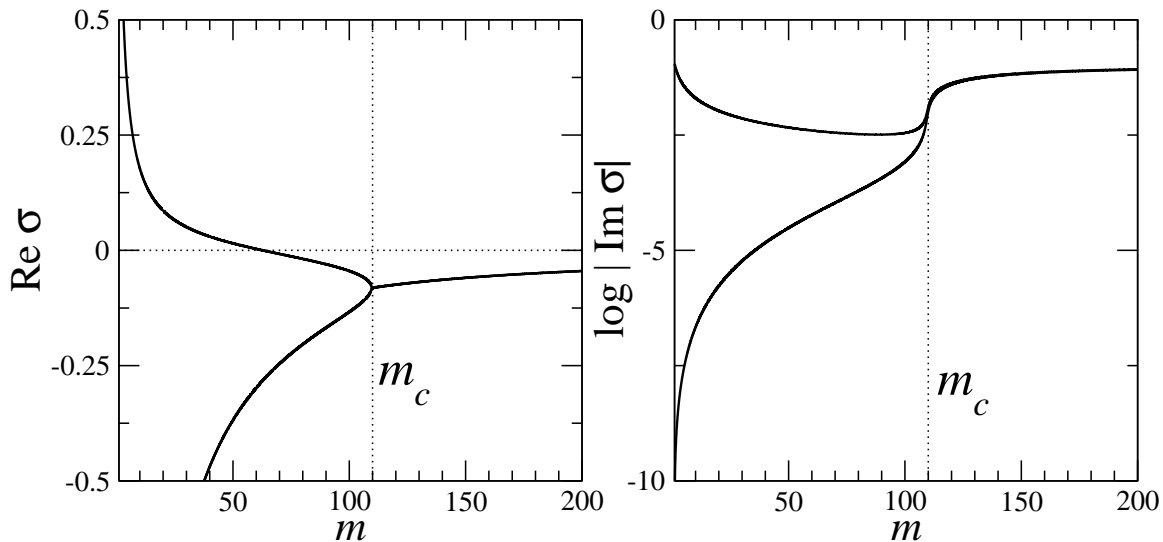


FIG. 2: Real (left panel) and imaginary parts (right panel) of the r-modes for $\mathcal{R} = 100$, $x_p = 0.1$ and a rotational lag $\Delta = 5 \times 10^{-4}$. Beyond a critical critical value for the azimuthal index, m_c , the modes are dynamically unstable. The onset of this instability is associated with (near) merger of the real part of the two frequencies. The absence of sign change of the imaginary part of the unstable branch shows the presence of a secular instability for smaller values of m .

Let us first see if we can find approximate solutions that demonstrate the behaviour seen in the numerical results. Returning to (41) and (42) we see that the two degrees of freedom (represented by U^m and u^m) only couple at order Δ . Since we are interested in

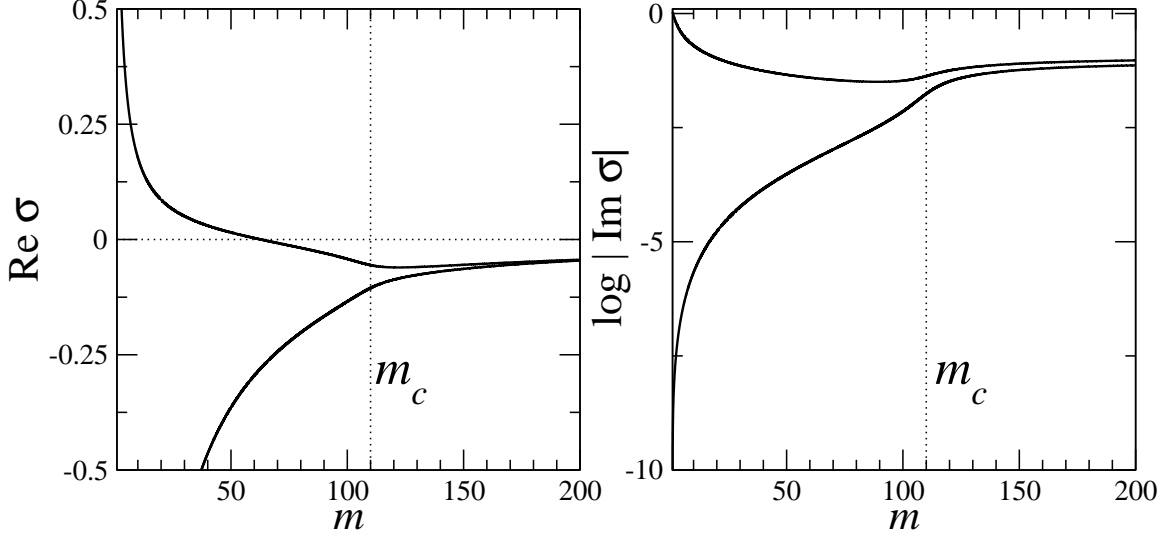


FIG. 3: Same as Fig. 2 but for $\mathcal{R} = 10$.

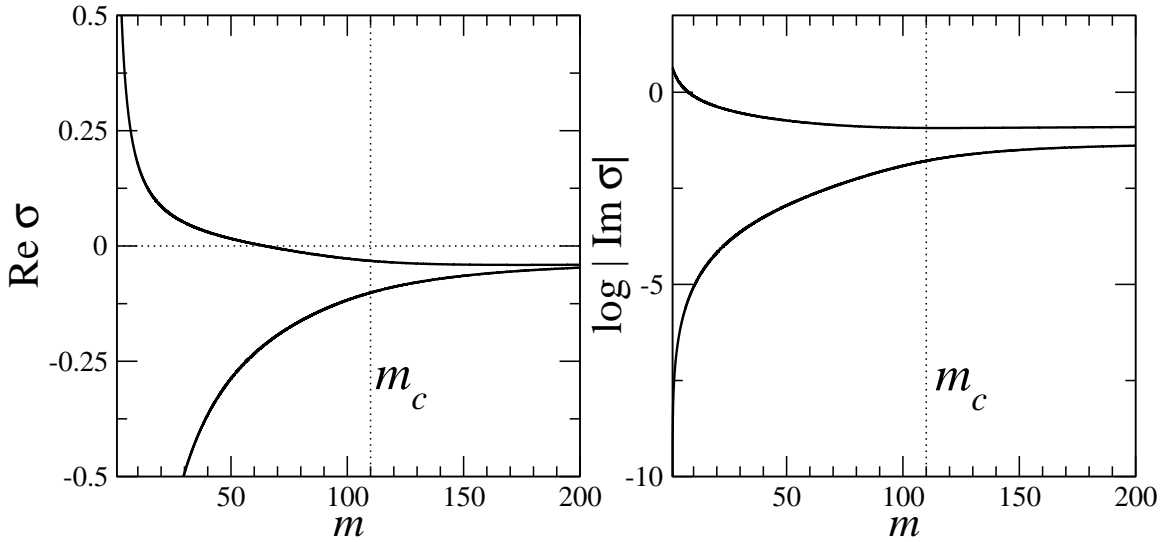


FIG. 4: Same as Fig. 2 but for $\mathcal{R} = 2$.

mode solutions for small Δ , this suggests that the solutions are either predominantly co- or counter-moving, depending on whether U^m dominates over u^m , or vice versa. Considering first the co-moving case, we assume that $U^m \neq 0$ and $u^m \approx 0$, which leads to

$$\sigma = \frac{1}{m+1} [2 - \Delta(1 - x_p)(m-1)(m+2)] \equiv \sigma_0 \quad (60)$$

At this level, the frequency is real and the modes are stable.

Meanwhile, in the counter-moving case we have modes with frequency

$$\sigma = \frac{1}{(1 - \bar{\varepsilon})(m + 1)} \left\{ 2(1 - \bar{\mathcal{B}}' + i\bar{\mathcal{B}}) - \Delta x_p(m - 1)(m + 2) + \bar{\varepsilon}\Delta \{ [m(m + 1) - 4]x_p + 2 \} \right. \\ \left. + m(m + 1)\Delta x_p(1 - \bar{\varepsilon})(\bar{\mathcal{B}}' + i\bar{\mathcal{B}}) - 2(1 - \varepsilon_n)(\bar{\mathcal{B}}' - i\bar{\mathcal{B}})\Delta \right\} \quad (61)$$

From this we see that the imaginary part of the frequency is proportional to

$$2 + m(m + 1)\Delta x_p(1 - \bar{\varepsilon}) + 2(1 - \varepsilon_n)\Delta$$

which suggests that the counter-moving modes tend to be stable, at least in the non-entrainment case. When the entrainment is accounted for, these modes may become unstable. In the short lengthscale limit, when $m^2 x_p \Delta \gg 1$ (corresponding to $m \gg 10^3$ or so for typical parameters), an instability is present as long as $\varepsilon_n > x_p$, which is not a particularly severe criterion.

Let us now consider the co-rotating modes at the next level of approximation. We have already seen from (60) that, to leading order in Δ , these modes are marginally stable, with frequency approximated by σ_0 . Yet, we know from the numerical results that an instability should be present for some range of \mathcal{R} , certainly $\mathcal{R} \geq 2$. Hence, we need to estimate the solution at the next order in Δ . To do this, we take

$$\sigma = \sigma_0 + \sigma_2 \Delta^2 \quad (62)$$

which leads to

$$\sigma_2 = \frac{(m - 1)(m + 2)}{2(m + 1)} \frac{x_p(1 - x_p)}{(\bar{\mathcal{B}}' - i\bar{\mathcal{B}})} [(m - 1)(m + 2) - m(m + 1)(\bar{\mathcal{B}}' + i\bar{\mathcal{B}})] \quad (63)$$

We are (primarily) interested in the imaginary part of the frequency. Since we know that an instability exists in the strong-coupling limit we note that this limit corresponds to $\bar{\mathcal{B}}' \approx 1/x_p$ and hence we have (to order $\bar{\mathcal{B}}$)

$$\text{Im } \sigma_2 = -\frac{(m - 1)(m + 2)}{2(m + 1)} x_p(1 - x_p) [m(m + 1)(2 - x_p) + 2x_p] \bar{\mathcal{B}} \quad (64)$$

We learn that these modes are *unstable* for *all* values of Δ . We also see that the growth rate scales as $1/\bar{\mathcal{B}}$ making this a secular instability. The estimate (64) establishes the presence of the instability for a wide range of parameters, and provides more detailed insight into the dependence on the parameters.

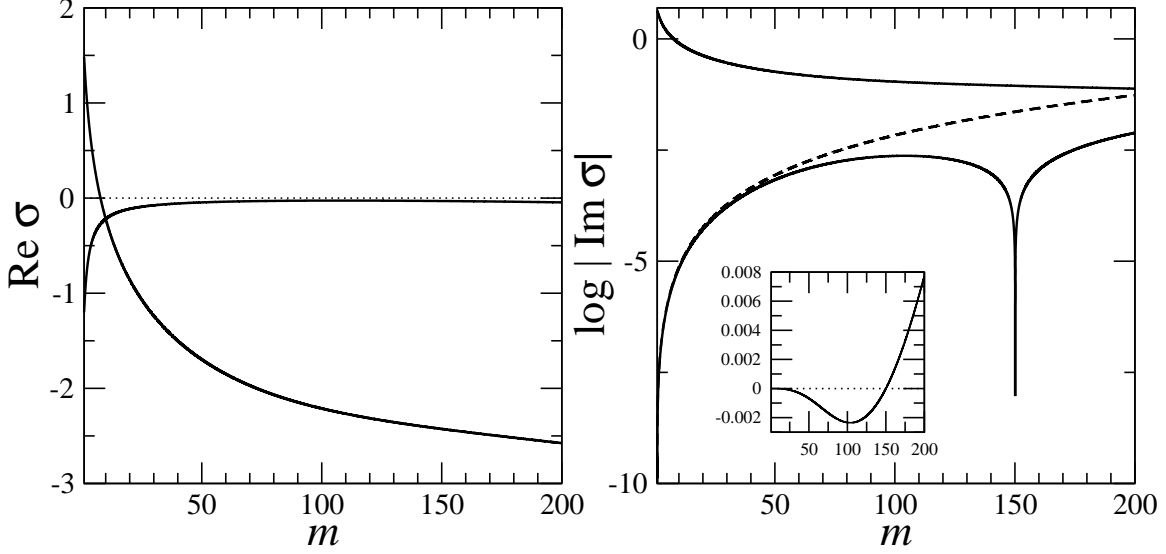


FIG. 5: Same as Fig. 2 but for $\mathcal{R} = 0.5$. The inset in the right panel shows the detailed behaviour of $\text{Im } \sigma$ as function of m . The dashed curve in the right-hand panel corresponds to the approximate solution (63), which is an accurate representation for low multipoles.

It is obviously relevant to establish what the critical value of \mathcal{R} may be. We can get an idea of this by working out where the imaginary part of (63) changes sign. This leads to

$$\mathcal{B}'_c = \frac{\mathcal{R}_c^2}{1 + \mathcal{R}_c^2} = \frac{(m-1)(m+2)}{2m(m+1)} x_p \quad (65)$$

For $\mathcal{R} \leq \mathcal{R}_c$ the system should be stable. It is easy to show that this is the case by considering the weak-coupling limit. Then we have $\bar{\mathcal{B}}' \sim \bar{\mathcal{B}}^2$ so the dominant behaviour will be

$$\text{Im } \sigma_2 = \frac{(m-1)^2(m+2)^2}{2(m+1)} x_p (1 - x_p) \frac{1}{\bar{\mathcal{B}}} \quad (66)$$

As expected, the modes are *always stable* in this limit. This is, of course, as expected.

Returning to the numerical results, the typical behaviour for $\mathcal{R}_c < \mathcal{R} < 1$ is similar to that shown in Fig. 5 (which corresponds to $\mathcal{R} = 0.5$). That is, for a given value of \mathcal{R} the instability is present for a range of multipoles, up to a critical value where the modes become stable. Above $\mathcal{R} = 1$ all modes are unstable.

We get a complementary view of the new instability by fixing the multipole m and varying \mathcal{R} . This leads to the results shown in Figures 6 and 7, for $m = 2$ and $m = 100$, respectively. These results demonstrate that the instability exists throughout the $\mathcal{R} \geq 1$ regime, and that it extends into the “weak-coupling” regime, as well. This is yet another demonstration of

the generic nature of the superfluid r-mode instability. It is notable that the approximation (64) is excellent for low values of m , see the right-hand panel of Fig. 6, but deteriorates as m increases. This is not surprising since, for large values of m one cannot simply neglect higher order terms in Δ as these may be multiplied by factors of m . In essence, the co- and counter-moving degrees of freedom are no longer neatly decoupled on shorter (angular) scales. Nevertheless, the approximation serves its purpose by illustrating the behaviour in an important part of parameter space.

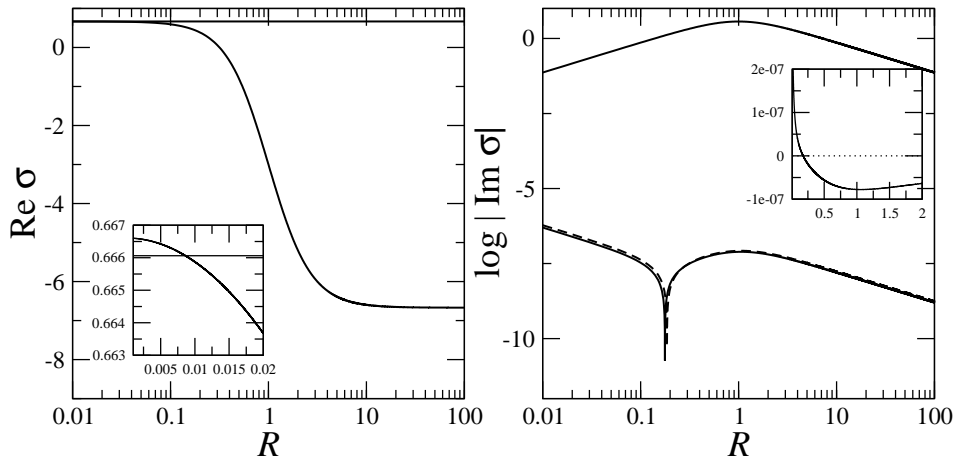


FIG. 6: Real (left panel) and imaginary parts (right panel) of the r-modes for $m = 2$, $x_p = 0.1$ and a rotational lag $\Delta = 5 \times 10^{-4}$. Unstable modes are present beyond a critical value of \mathcal{R} , see inset in the right panel. We compare the obtained imaginary part for the modes that become unstable to the estimate (63) (dashed curve in the right-hand panel). In this case, this is clearly a very good approximation. The inset in the left panel shows that the real parts of the mode frequencies cross at a low value of \mathcal{R} , seemingly unrelated to the onset of instability.

V. ASTROPHYSICAL CONTEXT: ACCOUNTING FOR SHEAR VISCOSITY

As suggested in [12], the superfluid instability discussed in the previous section could be relevant for astrophysical neutron stars, in particular glitching pulsars. A “minimum” requirement for this to be the case is that the instability grows fast enough to overcome the dissipative action of viscosity in neutron star matter.

A mature neutron star core is sufficiently cold to contain both superfluid neutrons and protons (recent evidence suggest that this is the case for a core temperature $T \lesssim 5 - 9 \times$

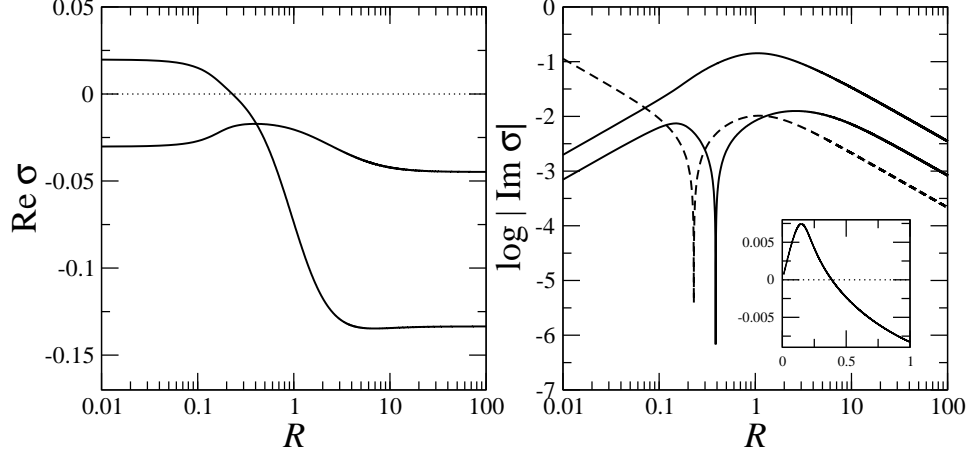


FIG. 7: The same as Figure 6, but for $m = 100$. In this case, (63) no longer provides a good approximation to the imaginary part.

10^8 K [29, 30]. Under these conditions the fluid motion is primarily damped by vortex mutual friction (which we have already accounted for, and which drives the instability we are considering) and shear viscosity due to electron-electron collisions [31]. Drawing on the considerable amount of work that has been done on the gravitational-wave driven r-mode instability [32], we can estimate the shear viscosity damping timescale using an energy-integral approach;

$$\tau_{\text{sv}} = \frac{E_{\text{mode}}}{\dot{E}_{\text{sv}}} \quad (67)$$

where E_{mode} is the mode energy and \dot{E}_{sv} is the shear viscosity damping rate. The damping timescale (67) can be easily calculated using the two-fluid r-mode results of the previous sections. However, as we are only interested in a rough estimate we use the result for ordinary single-fluid r-modes in a uniform density star [33] to approximate τ_{sv} . This leads to

$$\tau_{\text{sv}} = \frac{3}{4\pi} \frac{M}{\eta_{\text{ee}} R} \frac{1}{(2m+3)(m-1)} \approx \frac{1.3 \times 10^6}{m^2} \left(\frac{0.05}{x_{\text{p}}} \right)^{3/2} \frac{R_6^{7/2}}{M_{1.4}^{1/2}} T_8^2 \text{ s} \quad (68)$$

where $R_6 = R/10^6 \text{ cm}$ and $M_{1.4} = M/1.4 M_{\odot}$ represent the radius and mass of the star, respectively. The relevant shear viscosity coefficient ($\eta_{\text{ee}} = \rho_{\text{p}} \nu_{\text{ee}}$) has been taken to be [31]

$$\eta_{\text{ee}} = 1.5 \times 10^{19} \left(\frac{x_{\text{p}}}{0.05} \right)^{3/2} \rho_{14}^{3/2} T_8^{-2} \text{ g cm}^{-1} \text{ s}^{-1} \quad (69)$$

where $\rho_{14} = \rho/10^{14} \text{ g cm}^{-3}$ and $T_8 = T/10^8 \text{ K}$.

We are now in a position where we can compare the growth timescale, τ_{grow} , to that due to shear-viscosity damping, τ_{sv} . Such a comparison is provided in Figure 8 for modes

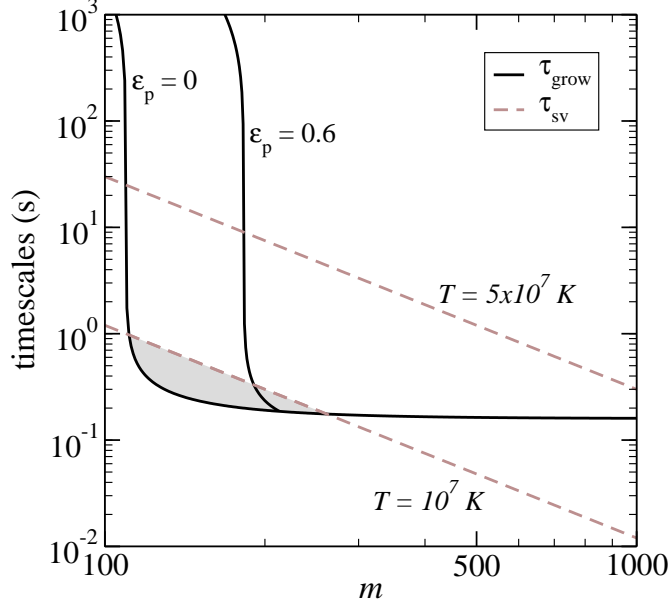


FIG. 8: The dynamical r-mode instability growth and viscous damping timescales τ_{grow} and τ_{sv} (from Eqns. (57) and (68), respectively) as functions of the multipole m for typical pulsar parameters: $P = 0.1$ s, $x_p = 0.1$ and strong drag $\mathcal{R} = 10^4$. The stellar mass and radius are fixed at the canonical values $M_{1.4} = R_6 = 1$. The shear viscosity damping rate τ_{sv} is shown for two core temperatures: $T = 10^7$ K and $T = 5 \times 10^7$ K. The spin-lag Δ is fixed to 5×10^{-4} and we show results for two values of the entrainment parameter, $\varepsilon_p = 0$ and $\varepsilon_p = 0.6$. The grey region indicates the range of unstable r-modes for $T = 10^7$ K.

exhibiting the dynamical instability (in the strong-coupling regime) and typical neutron-star parameters. The timescales are shown as functions of the multipole m , and we provide results for two choices of the entrainment parameter ε_p , cf. Fig. 1. The damping rate τ_{sv} is shown for two representative core temperatures $T = 10^7$ K and 5×10^7 K, representing mature neutron stars. Dynamically unstable superfluid r-modes exist for the range of m *above* the τ_{grow} curve but *below* the τ_{sv} curve. The results show that the τ_{grow} profile levels off (as a function of m) for $m \gtrsim m_c$ and that the instability can overcome the viscous damping for a range of scales. We also see that the entrainment has a small effect on the asymptotic behaviour of τ_{grow} but can significantly affect the critical multipole m_c . Finally, it is apparent that the range of unstable modes decreases as the star cools. This is an interesting observation since glitches are only seen in relatively young pulsars. The results in Figure 8 indicate that shear viscosity would prevent the instability from developing soon

after the star has cooled below 10^7 K. It is worth keeping in mind that the core temperature may remain above 10^8 K for (at least) the first 10^5 years of a pulsar's life [36].

The predicted spin-lag for the dynamical instability to set in also makes a connection with pulsar glitches seem plausible. Balancing the mode growth and the viscous damping, i.e., setting $\tau_{\text{grow}} = \tau_{\text{sv}}$, we find the critical spin lag Δ_c above which the instability is active. Combining (51) and (68) and setting $m = m_c$ we obtain

$$\Delta_c \approx 3.3 \times 10^{-5} \left(\frac{x_p}{0.05} \right)^{2/3} \left(\frac{P}{1 \text{ s}} \right)^{2/3} \left(\frac{m_p^*}{m_p} \right)^{-1/3} T_8^{-4/3} \quad (70)$$

This result was first derived in [12]. As discussed in that paper, the predicted critical lag compares well with the available data for large pulsar glitches. This could be an indication that large glitches are indeed triggered by the large m r-mode instability.

The results for the secular instability for smaller values of m are quite similar. In Fig. 9 we show results both for $m = 2$ and $m = 100$. In each case we see that unstable modes will be present above a certain temperature. Keeping in mind that the critical temperature for core superfluidity is expected to be below 10^9 K, while a typical glitching pulsar like the Vela is expected to have core temperature just above 10^8 K, these results make it seem plausible that the secular instability can become active in these systems. Whether astrophysical systems with \mathcal{R} in the required range for the instability exist is not clear at this point. Most work has focussed on smaller values, in which case the system would not exhibit the instability we have discussed here, but there have been suggestions of larger values [34]. It is also worth noting that a stronger mutual friction may help reconcile the discrepancy between our theoretical understanding of the r-mode instability with observed astrophysical systems [35].

VI. FINAL REMARKS

We have provided a more detailed analysis of the superfluid r-modes in a simple uniform density model with (solid body) differential rotation between the two components. As already discussed in [12], the results of this analysis are interesting, both conceptually and from the point-of-view of astrophysical applications. It is obviously interesting that the vortex-mediated mutual friction may lead to the presence of an instability. However, this is perhaps not surprising given the wealth of results relating to instabilities triggering superfluid

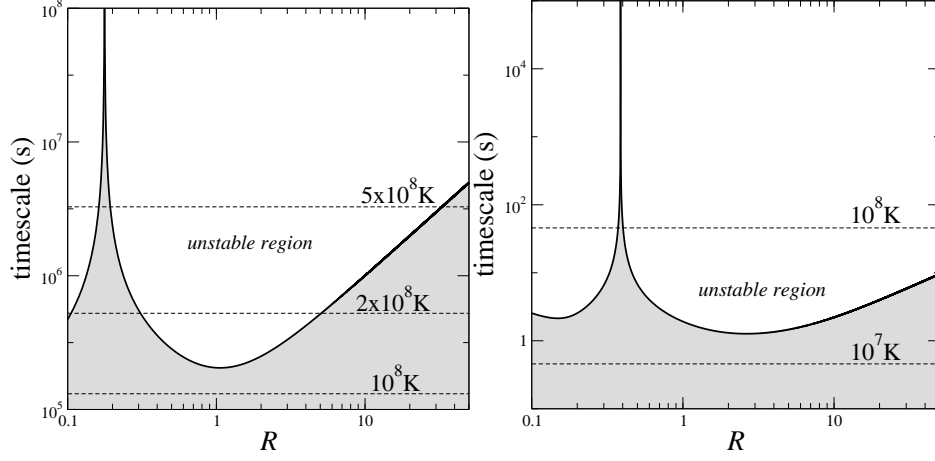


FIG. 9: The secular r-mode instability growth and viscous damping timescales τ_{grow} and τ_{sv} (obtained from the numerical solution to (43) and (68), respectively) as functions of \mathcal{R} for two multipoles: $m = 2$ (left panel) and $m = 100$ (right panel). The other parameters are the same as in Fig. 8: $P = 0.1$ s, $x_p = 0.1$ and $M_{1.4} = R_6 = 1$. The spin-lag Δ is fixed to 5×10^{-4} . The shear viscosity damping rate τ_{sv} is shown for various temperatures as indicated in each panel (dashed horizontal lines). The r-mode growth time is short enough for an instability to be present for a range of \mathcal{R} for temperatures characteristic of young neutron stars.

turbulence [37, 38] and previous results in the context of pulsar precession [39, 40], but the present analysis provides the first demonstration of this kind of instability for global mode oscillations. We are also breaking new ground by considering perturbations for background configurations with differential rotation. It is notable that, as soon as we allow for this extra degree of freedom the problem becomes richer.

A particularly interesting aspect of the results is the presence of both secular and dynamical instability behaviour in (more or less) distinct parts of parameter space. The behaviour that we have unveiled is summarized in the phase plane in Figure 10, that shows the unstable region in the $m - \mathcal{R}$ plane. As far as we are aware, the present analysis represents the first detailed study of a problem that has secularly unstable modes entering a regime where they become dynamically unstable. The associated behaviour is, in many way, predictable. For example, instead of having modes becoming dynamically unstable as real-valued frequency pairs merge and form complex conjugate pairs, we now have dynamical instability behaviour associated with “near misses” in the complex frequency plane. Our results suggest that dynamical instability only results provided that the damping of the modes is not too large (in

our case $\mathcal{R} \geq 10$ or so). To improve our understanding further, we need to consider the necessary and sufficient criteria for the superfluid instability to operate. This is a challenging problem but it seems likely that one could make progress by adding the perturbed mutual friction force to the results in [43].

An interesting analogous problem concerns the $l = m = 2$ bar-mode in rotating neutron stars. This mode is known to become secularly unstable due to the emission of gravitational waves well before (along a sequence with increasing degree of differential rotation) it becomes dynamically unstable, see [23] for a review and [41] for recent work. The behaviour of that instability may be quite similar to that of the superfluid problem we have discussed here. If this is the case, then a key question concerns whether there always is a dramatic change in gravitational-wave emission rate before and after the critical parameter for onset of the dynamical instability is reached. In the bar-mode problem there is also another class of instability, commonly referred to as the low T/W instability [42]. We have no evidence for an analogous instability in the present problem.

Even though we have not discussed possible astrophysical repercussions in any detail, it is clear that the potential link with the unresolved problem of radio pulsar glitches provides strong motivation for further work on this problem. Of course, we cannot at this point really tell how relevant the new r-mode instability is in this context. In order to act in an astrophysical system, the instability must be robust enough to remain once we account for the star's magnetic field and the elastic crust. These features are likely to affect the instability considerably, but more work is required if we want to quantify what the effects may be. The two-stream instability mechanism is sufficiently generic that it would be remarkable if it would cease to operate in more complex settings, but it could be that the instability threshold moves out of reach for a real system. At this point, we cannot say. There is, however, fresh evidence supporting the existence of short wavelength superfluid instabilities in the presence of a magnetic field and/or an elastic crust, see [44, 45]. The exact relation between these instabilities and our r-mode instability is still unclear, apart from the fact that both require vortex mutual friction to operate. The secular instability behaviour is obviously also worthy of further attention. In particular, since it is relevant also for large scale modes, including the lowest multipoles that are the most important from the gravitational-wave point-of-view. The problem is clearly extremely interesting and well worth returning to in the future.

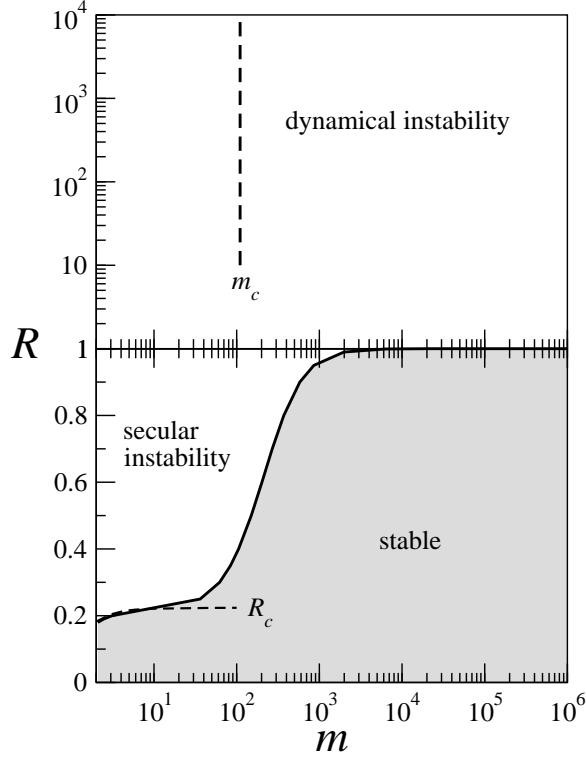


FIG. 10: Summary of the parameter space \mathcal{R} vs m , indicating the different regions of instability for $x_p = 0.1$ and $\Delta = 5 \times 10^{-4}$. Dashed curves show the critical multipole m_c where the behaviour changes from secular to dynamical instability on the strong coupling regime (upper panel), and the estimated critical drag \mathcal{R}_c from (65) where the secular instability sets in for low m -multipoles (lower panel).

Acknowledgments

NA is supported by STFC in the UK. KG is supported by the Ramón y Cajal Programme in Spain.

-
- [1] Radhakrishnan, V., and Manchester, R.N. , Nature, 222, 228 (1969)
 - [2] Reichley, P.E., and Downs, G.S. , Nature, 222, 229 (1969)
 - [3] Lyne, A.G., Shemar, S.L., and Smith, F. Graham, MNRAS 315, 534 (2000)
 - [4] Espinoza, C.M., Lyne, A.G., Stappers, B.W., and Kramer, M., MNRAS 414, 1679 (2011)
 - [5] Sidery, T., Passamonti, A., and Andersson, N., MNRAS 405, 1061 (2010)

- [6] Pizzochero, P.M., Ap. J. Lett. 743, L20 (2011)
- [7] Warszawski, L., and Melatos, A., MNRAS 415, 1611 (2011)
- [8] Warszawski, L., Melatos, A., and Berloff, N.G., Phys. Rev. B 85, 104503 (2012)
- [9] Haskell, B., Pizzochero, P.M., and Sidery, T., MNRAS 420, 658 (2012)
- [10] Baym, G., Pethick, C., and Pines, D., Nature, 224,872 (1969)
- [11] Anderson, P.W., and Itoh, N. Nature, 256, 25 (1975)
- [12] Glampedakis, K., and Andersson, N., Phys. Rev. Lett. 102, 141101 (2009)
- [13] Andersson, N., Comer, G.L., and Prix, R., Phys. Rev. Lett. 90, 091101 (2003)
- [14] Andersson, N., Comer, G.L., and Prix, R., MNRAS 354, 101 (2004)
- [15] Glampedakis, K., Andersson, N., and Samuelsson, L., MNRAS 410, 805 (2011)
- [16] Alpar, M.A., Langer, S.A., and Sauls, J.A., Ap. J. 282, 533 (1984)
- [17] Mendell, G., Ap. J. 380, 530 (1991)
- [18] Andersson, N., Sidery, T., and Comer, G.L., MNRAS 368, 162 (2006)
- [19] Andersson, N. and Comer, G.L., MNRAS 328, 1129 (2001)
- [20] Andersson, N., Glampedakis, K., and Haskell, B., Phys. Rev. D 79, 103009 (2009)
- [21] Andersson, N., and Kokkotas, K.D., Int. J. Mod. Phys. D 10, 381 (2001).
- [22] Lockitch, K.H. , and Friedman, J.L., Ap. J., 521, 764 (1999)
- [23] Andersson, N., Class. Quantum Grav. 20, R105 (2003)
- [24] Abney, M., Epstein, R.I. and Olinto, A.V., Ap. J. Lett. 466, L91(1996)
- [25] Donnelly R. J., *Quantized Vortices in Helium ii* (Cambridge Univ. Press, Cambridge, 1991)
- [26] Glaberson W. I., Johnson W.W., and Ostermeier R.M., Phys. Rev. Lett., 33, 1197 (1974)
- [27] Sidery, T., Andersson, N., and Comer, G.L., MNRAS 385, 335 (2008)
- [28] Prix, R., Comer, G.L., and Andersson, N., Astron. Astrophys. 381, 178 (2002)
- [29] Page, D., Prakash, M., Lattimer, J.M., and Steiner, A.W., Phys. Rev. Lett. 106, 081101 (2011)
- [30] Shternin, P.S., Yakovlev, D.G., Heinke, C.O., Ho, W.C.G., and Patnaude, D.J., MNRAS 412, L108 (2011)
- [31] Andersson, N., Comer, G.L., and Glampedakis, K., Nucl. Phys. A 763, 212 (2005)
- [32] Andersson, N. and Kokkotas, K.D., Int. J. Mod. Phys. D., 10, 381 (2001)
- [33] Kokkotas, K.D., and Stergioulas, N., Astron. Astrophys. 341, 110 (1999)
- [34] Sedrakian, A.D., and Sedrakian, D.M., Ap. J. 447, 305 (1995)
- [35] Ho, W.C.G., Andersson, N., and Haskell, B., Phys. Rev. Lett. 107, 101101 (2011)

- [36] Ho, W.C.G., Glampedakis, K., and Andersson, N., MNRAS 422, 2632 (2012)
- [37] Andersson, N., Sidery, T., and Comer, G.L., MNRAS 381, 747 (2007)
- [38] Peralta, C., Melatos, A., Giacobello, M., and Ooi, A., Ap. J. 651, 1079 (2006)
- [39] Glampedakis, K., Andersson, N., and Jones, D.I., Phys. Rev. Lett. 100, 081101 (2008)
- [40] Glampedakis, K., Andersson, N., and Jones, D.I., MNRAS 394, 1908 (2009)
- [41] Manca, G.M., Baiotti, L., DePietri, R., and Rezzolla, L., Class. Quantum Grav., 24, S171 (2007)
- [42] Watts, A. L., Andersson, N., and Jones, D. I., Ap. J. Lett. 618, L37 (2005)
- [43] Andersson, N., Comer, G.L., and Grosart, K., MNRAS 355, 918 (2004)
- [44] Link. B., MNRAS, 421, 2682 (2012)
- [45] Link. B., MNRAS, 422, 1640 (2012)